International Journal of Electrical and Electronics Engineers
Volume 15, Issue No. 02, July-Dec 2023
ISSN (O) 2321-2055
ISSN (P) 2321 -2045

Study of cosmic ray intensity variation in relation to solar activity for Sunspot Cycle 23 to 24

Brijesh dwivedi

Phd Scholler APSU Rewa

Email - bwivedi 233@gmail.com

Dr.Achyut pandey

HOD physics and head of computer science TRS college rewa

Email- achyut.pandey9@gmail.com

C.M.Tiwari

Department of Physics, APS University rewa (M.P.)

Email-cmtiwari_2005@yahoo.com

ABSTRACT

In this paper, we concentrate on the cosmic vast beam (GCR) varieties over the sun powered cy-cles 23 and 24, with estimations from the NASA's Pro/CRIS instrument and the ground-based neutron screens (NMs). The outcomes show that the most extreme GCR powers of weighty cores ($5 \leq Z \leq 28$, 50∼500 MeV/nuc) at 1 AU during the so-lar least in 2019-2020 break their past records, surpassing those kept in 1997 and 2009 by ∼25% and ∼6%, separately, and are at the most elevated levels since the space age. Notwithstanding, the pinnacle NM count rates are lower than those in late 2009. The distinction between GCR powers and NM count rates actually still needs to be made sense of. Besides, we track down that the GCR adjustment climate during the sunlight based least P24/25 are fundamentally not the same as past sun powered minima in a few perspectives, including

amazingly low sunspot numbers, incredibly low tendency of the heliospheric current sheet, uncommon coronal mass launches, powerless interplanetary attractive field and choppiness. These progressions are helpful for decrease the degree of sun powered regulation, giving a plau-sible clarification to the record-breaking GCR forces in interplanetary space.

Keyword :- SW, CMEs, cosmic, sun powered, Galactic, Rays, Solar Cycles, Variations

1. INTRODUCTION

Because of the supersonic extension of the sunlight based breeze (SW), the heliosphere resembles a goliath lopsided air pocket loaded up with different fiery particles. These particles are the predominant wellspring of room radiation climate, representing a huge danger to the ordinary activity of rocket and high-elevation airplane, and the wellbeing of space travelers and flight faculty (e.g., Mertens and Slaba 2019). Sun oriented fiery particles (SEPs), cosmic enormous beams (GCRs) and peculiar astronomical beams (ACRs) are the three regularly seen vigorous particles in the interplanetary space.

SEPs, otherwise called sun based vast beams, are the particles starting from the Sun with energies going from a many keV to a few GeV. They are regularly connected with coronal mass discharges (CMEs) and sun based flares. It is broadly acknowledged that CME-driven shock is a fundamental site for speeding up sun powered vivacious particles (e.g., Hu et al. 2017, 2018; Fu et al. 2019; Ding et al. 2020). GCRs are much of the time viewed as a steady foundation, and are accepted to begin from the cosmic explosion leftovers (SNRs) and advanced quickly by cosmic explosion impact shocks driven by extending SNRs. This is affirmed by perceptions and mathematical recreations (Aharonian et al. 2007, 2011; Ptuskin et al. 2010). During the tranquil periods, the motions of some inestimable beam species with high first ionization possibilities, including H, He, C, N, O, Ne and Ar, are essentially higher than the foundation GCRs, i.e., abnormal grandiose beams (Hovestadt et al. 1973; McDonald et al. 1974; Hasebe et al. 1997). A traditional clarification of ACRs is that they start from the interstellar medium, in which the impartial particles float into the heliosphere and become separately ionized by the sun powered breeze or the bright radiation which are in this way advanced to energies over 10 MeV/nuc, generally happening at or close the heliospheric end shock (Mewaldt et al. 1993; Cummings and Stone 2007; Gloeckler et al. 2009). New systems for ACR speed increase have been advanced (e.g., Giacalone et al. 2012, and references in that, for example, Zhao et al. 2019 proposed that ACR protons are advanced in the

heliosheath through reconnection processes. Concentrating on the idea of fiery particles gives understanding into the speed increase instruments and the vehicle processes between the sources and the spectators. At the point when GCR particles from the space (the purported essential grandiose beam) experience the Earth and infiltrate the World's air, they interface with barometrical molecules and produce fountains of optional particles (e.g., Mishev et al. 2014). The optional particles (dominatingly neutrons and muons at the ground level) can be estimated by the ground-based neutron screens (NMs) and muon indicators once showing up at the outer layer of the Earth. The historical backdrop of neutron screens can be followed back to the 1950s (Bieber 2013). The blend of GCR powers from in-situ rockets and GCR count rates from NM stations is useful to portray a somewhat complete image of enormous beams (CRs). Moreover, the cosmogenic isotope kept in tree rings and ice centers can broaden our

comprehension of GCRs throughout a more drawn out time scale (e.g., Owens and Forsyth 2013).

The vehicle of vast beams all through the heliosphere is fundamentally impacted by the huge scope sunlight based breeze stream and the tempestuous interplanetary attractive field implanted in it, altogether alluded to as "sun powered balance". Four significant adjustment processes have been very much portrayed by the Parker transport condition (Parker 1965), including slope and curve floats, dissemination through the unpredictable interplanetary attractive field (IMF), convection in the outspread extending sun based breeze, and adiabatic deceleration (or adiabatic energy misfortune) (e.g., Sabbah 2000; Zhao and Zhang 2015; Ihongo and Wang 2016; Zhao et al. 2018). Common estimations give direct proof to assessing their general job in influencing vast beam engendering throughout the course of recent many years (K'ota 2013), however the mathematical recreation of enormous beam transport is as yet an exceptionally difficult undertaking. The sunlight based attractive extremity (ordinarily depicted as [qA], where [q] signifies a decidedly charged molecule) is a vital calculate regulating infinite beam forces. Generally, the decidedly charged particles float internal along the heliospheric current sheet (HCS) when the heliospheric attractive field at the north pole focuses internal (negative extremity, $qA < 0$) and the charged particles float outward along the HCS when the heliospheric attractive field focuses outward at the north pole (positive extremity, $qA > 0$) (e.g., Jokipii and Thomas 1981; Belov 2000; Thomas et al. 2014). The 22-year heliomagnetic

cycle (additionally called Sound cycle) brings about the exchanging sharp (negative extremity, $qA < 0$) and level bested (positive extremity, $qA > 0$) state of grandiose beam power (McDonald et al. 2010).

International Journal of Electrical and Electronics Engineers
Volume 15, Issue No. 02, July-Dec 2023
ISSN (O) 2321-2055
ISSN (P) 2321 -2045

In late 2009, both the GCR forces estimated from close Earth rockets and the GCR count rates estimated from ground-based NM stations arrived at their then all-time most extreme levels (e.g., McDonald et al. 2010; Leske et al. 2013). Around then, the heliospheric climate was strange in a few perspectives, including debilitated interplanetary attractive field and disturbance level, diminished sun based breeze dynamic tension, and delayed sun powered least (Mewaldt et al. 2010). The little extent of the IMF causes higher molecule float speeds, and the debilitated IMF disturbance prompts bigger molecule mean free ways (MFPs) in the sun based least 2009 than those in its past sun powered minima. These bizarre interplanetary ways of behaving would lessen the degree of GCR regulation and add to the startling high GCR powers in 2009. As detailed, the sun powered cycle 24 was the most vulnerable in extent in the space age (Hajra 2021), and it likewise displayed a few strange signs, for example, diminished sunspots (particularly enormous spots) (Chapman et al. 2014), diminished coronal mass discharge occasions (Wang and Colaninno 2014), and extremely smoothed HCS. The sun oriented movement is by all accounts going through a time of "fantastic least" (Jiang and Cao 2018; Upton and Hathaway 2018; Gon¸calves et al. 2020). Previous examinations have anticipated that the pinnacle of the GCR powers in the sun based least 24/25 (from this point forward sunlight based least P24/25) would surpass or near the level kept in 2009-2010 (e.g., Strauss and Potgieter 2014; Kuznetsov et al. 2017; Fu et al. 2020).

The fundamental inspiration of this paper is to give a nearby reevaluation of the GCR varieties during the progressive sunlight based cycles 23 and 24, with specific interest to the most extreme GCR forces saw at 1 AU during the sun powered least P24/25 age. The paper is built as follows. In Area 2, we depict the wellsprings of the dataset used in this work. In Area 3, we present the observational aftereffects of GCRs and research the potential purposes behind the record-breaking GCR forces in 2019-2020 saw at 1 AU. We sum up this work in Area 4.

2. DATA DESCRIPTION

Sun oriented lively particles and strange astronomical beams don't add to the powers estimated by Expert/CRIS, and subsequently they don't partake in the accompanying examination.

GCR powers at 1 AU are seen by the in-situ Grandiose Beam Isotope Spectrometer (CRIS) instrument on board the NASA's High level Sythesis Voyager (ACE) shuttle, and GCR count rates at the ground level are checked by the five neutron screen stations recorded in Table 1.

The Pro space apparatus was sent off on 25 August 1997 and has been constantly observing sun based breeze plasma, interplanetary attractive fields and fiery particles (counting both sun oriented vigorous particles and enormous beams) at the Sun-Earth L1 Lagrange point (Stone et al. 1998) for almost 24 years, traversing the sunlight based cycles 23 and 24. The CRIS instrument was intended to gauge GCR forces of 24 weighty species (from boron to nickel, inside the energy range 50-500 MeV/nuc). Regardless of the low overflow (∼1%), the high nuclear number and energy cores convey bountiful data of
the beginning of the grandiose beams, and are of exceptional importance to space radiation (e.g., Zhao and Qin
2013; Fu et al. 2020). With the huge mathematical acknowledgment and high charge and mass goal, the CRIS instrument records the most nitty gritty and measurably critical GCR information to date (Stone et al. 1998). Verifiable Expert/CRIS perceptions are indisputable and openly available from the ACE Science Place (ASC) by means of http://www.srl.caltech.edu/ACE/ASC/index.html. Here we apply the rethought level-2 CRIS items, and these information are coordinated into 27-day Bartels revolution midpoints for the period from 25 August 1997 through 31 October 2020.

Pressure-rectified and 27-day found the middle value of GCR count rates are gotten from five neutron screen stations (HRMS, JUNG, NEWK, OULU, THUL) throughout the 1968-2020 time span. The definite data of the five NM stations is given in Table 1, where Pc is the neighborhood geomagnetic cutoff unbending nature of every NM station, the trademark energy (i.e., the middle energy) EM is characterized

International Journal of Electrical and Electronics Engineers
Volume 15, Issue No. 02, July-Dec 2023
ISSN (O) 2321-2055
ISSN (P) 2321 -2045

so vast beams with energy higher (or lower) than EM add to half of the locator's counting rate (Usoskin et al. 2008; Zhao and Zhang 2016). All information are obtained from the Neutron Screen Information Base (NMDB, http://www01.nmdb.eu/).

The month to month mean sunspot number (SSN) is acquired from the Sun based Impacts Information Examination Center (WDC-SILSO, http://www.sidc.be/). The SW speed (Vsw), the SW dynamic strain (Pd), the IMF greatness (B) and the root mean square variety in the vector IMF (δB) are obtained from the OMNIWeb databasde (https://omniweb.gsfc.nasa.gov/ow.html). The HCS slant point and

the mean sun powered polar attractive field strength are acquired from the Wilcox Sun oriented Observatory information base (http://wso.stanford.edu/). The mean polar field is characterized as (N − S)/2, where N is the polar field strength at the northern pole, S is the polar field strength at the southern pole. The radiance CME records

are gathered from the SOHO/LASCO Radiance CME index (https://cdaw.gsfc.nasa.gov/CME list/corona/halo.html), and the yearly CME rates are from Prickly plant CME inventory (http://www.sidc.be/cactus/). Also, the GCR radiation portion rates close to the lunar surface are estimated by the Infinite Beam Telescope for the Impacts of Radiation (Pit) instrument on board the Lunar Surveillance Orbiter (LRO) and are accessible at https://pit web.sr.unh.edu/. Note that except if expressly expressed in any case, the previously mentioned information are all handled as 27-day normal.

Table 1. List of the neutron monitor stations used in this work

NM Station	Abbrev.	Longitude (deg)	Latitude (deg)	Altitude (m)	P_c (GV)	E_M (GeV)
Hermanus	HRMS	19.22	−34.42	26	4.58	12.67
Jungfraujoch	JUNG	7.98	46.55	3570	4.49	12.58
Newark	NEWK	-75.75	39.68	50	2.40	10.99
Oulu	OULU	25.47	65.05	15	0.81	10.30
Thule	THUL	-68.7	76.5	26	0.30	10.17

NOTE—P_c is the NM's local geomagnetic cutoff rigidity, E_M is the median energy of each NM stationand is defined as: $E_M = 0.0877 \cdot P_c^2 + 0.154 \cdot P_c + 10.12$ (Jämsén et al. 2007; Usoskin et al. 2008).

3. RESULTS AND DISCUSSIONS

The SSN perceptions uncover that the sun oriented action has been industriously declining since the mid 1980s. As displayed in Figures 1 and 2(a), the greatest smoothed SSNs of sun based burns 21 through 24 are 232.9, 212.5, 180.3, and 116.4, separately, showing a noticeable decrease in the sun powered cycle plentifulness. GCR transport in the heliosphere is delicate to differing sunlight based action. An extraordinary sun oriented action (like CME and sun based flare) can set off a progression of room weather conditions impacts and really keep GCR particles from entering the nearby planet group (solid sun powered tweak), while a tranquil Sun is conductive to improve GCR transitions as a result of the debilitated balance level. Then, we

survey the varieties of the sun oriented breeze and interplanetary boundaries from sun powered cycles 20 to 24 in Subsection 3.1; GCR observational outcomes, remembering GCR forces for interplanetary space and GCR counts at the ground level, are shown in Subsection 3.2; in Subsection 3.3, we explore how the internal heliospheric climate

International Journal of Electrical and Electronics Engineers
Volume 15, Issue No. 02, July-Dec 2023
ISSN (O) 2321-2055
ISSN (P) 2321 -2045

impacts the GCR force, with an accentuation on the record-breaking transitions during the sun based least P24/25; in Subsection 3.4, we call attention to an unexpected plunge in the GCR force during the slipping period of the sun oriented cycle 24 and give a short examination of the potential causes; the deliberate cosmic vast radiation dosages on the lunar surface are displayed in Subsection 3.5.

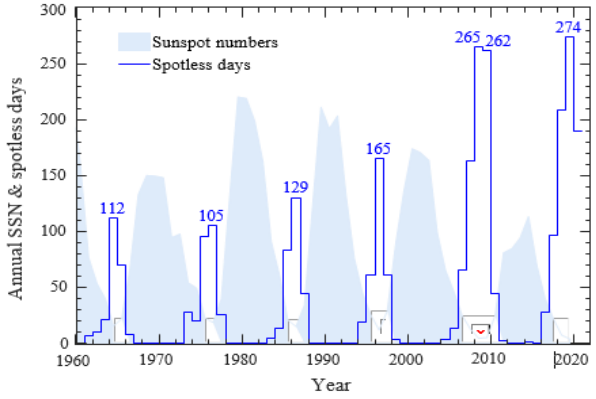

3.1. A glance of Solar Cycles 20–24

Sunspots were first seen by a telescope in the mid 1600s, and the consistent day to day perceptions started at the Zurich Observatory in the year 1849. The quantity of sunspots changes intermittently with time and shows a noteworthy semi long term cycle, which is presently generally perceived as a delegate of sunlight based action. In Figure 1, a striking element is that the most extreme sufficiency of sun powered cycle has been diminishing since the sun based cycle 21, and the as of late complete sun oriented cycle 24 is recorded to be

the most fragile one in the period of human space investigation (Hajra 2021). Moreover, there are absolutely 274 days without sunspots in the year 2019, which is the most in the beyond a long time (since the year 1914). The exceptionally tranquil sun powered least offers us a potential chance to dive deep into the circumstances winning in the past stupendous minima periods, like the Maunder Least (1645-1715) and the Dalton Least (1790-1830).
In Figure 2, we present the varieties of the sun oriented breeze/interplanetary boundaries in boards (b)- (f) and the deliberate NM include rates in board (g). A few notable highlights of the heliosphere and GCRs should be visible from these boards. (1) Both the HCS slant point, the IMF strength B and its disturbance δB (i.e., root mean square of vector IMF) are decidedly corresponded with SSN; (2) the GCR count rates at the ground level are contrarily connected with SSN; (3) the sun powered attractive field switches its extremity like clockwork, to be specific, 22-year heliomagnetic cycle (or Sound cycle); (4) the option crested (negative extremity, $qA < 0$) and level (positive extremity, $qA > 0$) states of NM count rates during progressive sun based minima periods is generally an indication of the Sun's polar attractive field inversion, and the greatest NM count rate during $qA > 0$ cycles (1977, 1997, 2019) is roughly 3% lower than that during $qA < 0$ cycles (1987, 2009).

3.2. Galactic Cosmic Rays during the Solar Cycle 24

Feeble sun based movement is supposed to diminish GCR adjustment level and permits more GCR particles to enter the internal heliosphere. Common GCR perceptions will be useful to feature the surprising heliospheric conditions during the incredibly peaceful sun based least P24/25. Not the same as the ground-based NM count rates, the perception of GCRs in space is short and frequently broken, however those early vast beam records (preceding the send off of Pro space apparatus) in interplanetary space can be remade from a few different satellites or the cutting edge cutting edge mathematical models, (for example, the CRE'ME model and the Badhwar-O'Neill model). Figure 3

International Journal of Electrical and Electronics Engineers
Volume 15, Issue No. 02, July-Dec 2023
ISSN (O) 2321-2055
ISSN (P) 2321 -2045

shows the lengthy GCR force profiles from 1970 to 2020, in which we look at the iron powers from Expert/CRIS with those from Demon - 8 in board (a), the carbon forces from Pro/CRIS with the helium powers from Devil - 8 in board (b), and the oxygen forces from Pro/CRIS with the BON2020 reproductions in board (c). In Figure 3(a), the GCR count rates from NEWK station are likewise plotted as a pattern. The pinnacle esteem

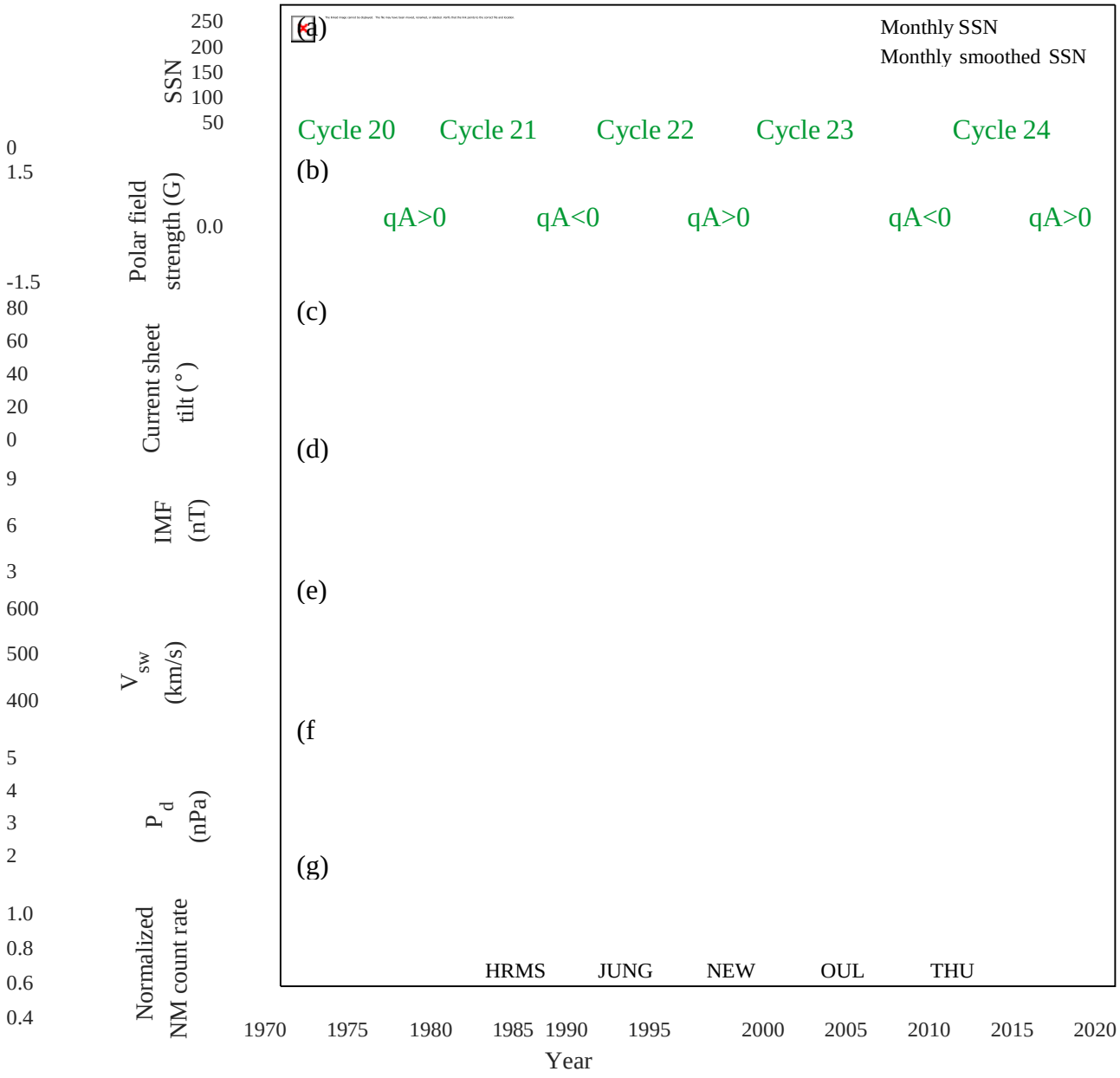

Figure27-day normal sunlight based breeze/interplanetary boundaries from January 1, 1968 to October 31, 2020. (a) Sunspot number. (b) Mean sun oriented polar field strength. (c) HCS Slant point. (d) IMF extent B and its root mean square δB. (e) Sun oriented breeze speed Vsw. (f) Sun oriented breeze dynamic tension Pd. (g) Strain revised neutron screen count rates (standardized to the sun based least P23/24 and increased by inconsistent variables for recognizing various stations). The shown attractive field extremity in board (b) relates to that at the northern pole. The upward ran line means the age of sun powered least.

of GCR forces at 1 AU in late 2009 was recently answered to be the most noteworthy in the space age 2.

International Journal of Electrical and Electronics Engineers
Volume 15, Issue No. 02, July-Dec 2023
ISSN (O) 2321-2055
ISSN (P) 2321 -2045

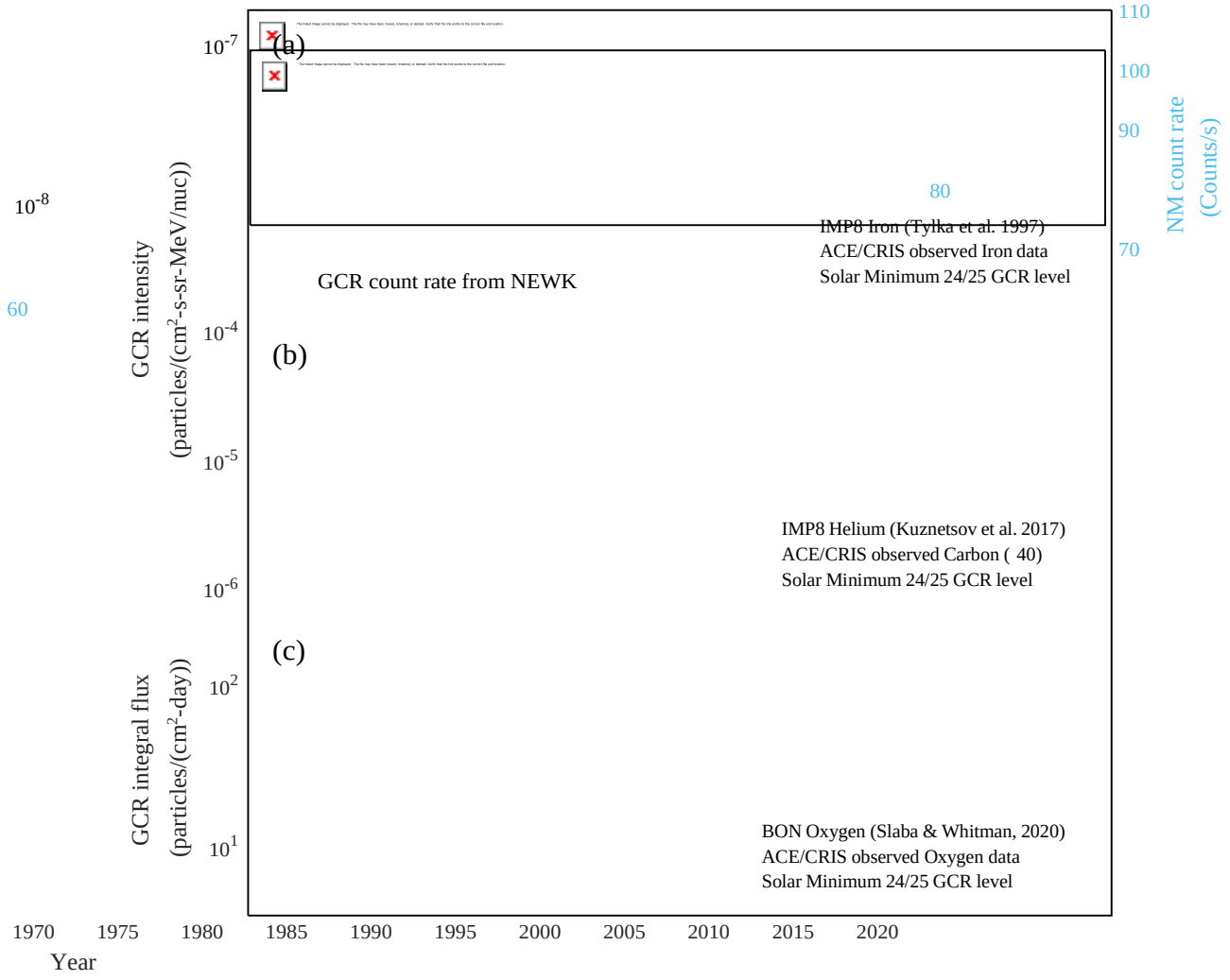

Figure 3. Secular variations of GCR intensities in interplanetary space and NM count rates. (a) GCR iron intensities from *ACE* /CRIS at 129.1–428.7 MeV/nuc (*red curve*) and from *IMP*-8 at 97.1–432 MeV/nuc (*black dots*, adapted from Tylka et al. 1997), compared with Newark GCR count rates (*cyan curve*, *right axis*). (b) GCR carbon intensities from *ACE* /CRIS at 184.8–200.4 MeV/nuc (*red curve*), compared with GCR helium intensities from *IMP8* /MED at ~265 MeV/nuc (*black curve*, adapted from Kuznetsov et al. 2017). (c) 69.4–237.9 MeV/nuc integral oxygen fluxes from *ACE* /CRIS (*red curve*), compared with the BON2020 modelled fluxes (*black curve*, adapted from Slaba & Whitman 2020). The horizontal dashed line marks the peak GCR intensity in the solar minimum $P_{24/25}$.

(McDonald et al. 2010; Mewaldt et al. 2010; Lave et al. 2013; Leske et al. 2013), but it is obvious that the maximum GCR intensities reach new heights during the solar minimum $P_{24/25}$, as depicted by the horizontal dashed line in Figure 3. The recent anomalous high GCR intensities at 1 AU are essentially a response to the unusual changes in the heliosphere, which will be further discussed in Subsection 3.3. Figures 4(a)–(c) plot the 27-day averaged *ACE* /CRIS GCR intensities over the solar cycles 23 and 24. Panel (a) shows the GCR intensities of element oxygen at seven energy bins, panel (b) the intensities of twelve selected species (C, O, Ne, Mg, Si, S, Ar, Ca, Ti, Cr, Fe, Ni), and panel (c) the averaged intensities of these twelve species. For comparison purpose, all profiles are normalized to the solar minimum $P_{23/24}$. It is clearly noted that the GCR intensities at 1 AU in late 2009 are much higher than those in 1997–1998 but slightly lower than

International Journal of Electrical and Electronics Engineers
Volume 15, Issue No. 02, July-Dec 2023
ISSN (O) 2321-2055
ISSN (P) 2321 -2045

those during the solar minimum $P_{24/25}$. The peak value of GCR intensities in the solar minimum $P_{24/25}$ is ~25% higher than that in the solar minimum $P_{22/23}$ and ~6% higher than that in the solar minimum $P_{23/24}$.

Figure 4(d) plots the 27-day averaged NM count rates from 1997 to 2020. Similar to the GCR intensity profiles, NM count rates also reach the highest level in late 2009 (Moraal & Stoker 2010), revealing that both low (<1 GeV) and high energy (several GeV) GCR particles have more chances to reach the Earth during the solar minimum $P_{23/24}$ (Mewaldt et al. 2010). However, the peak value of NM count rates in 2019–2020 does not exceed its 2009 level, which is not in accord with the observed GCR intensities in interplanetary space. The ground-based NM station only observes the high-energy GCRs (several GeV) as a consequence of the shielding effects from the Earth's magnetosphere and atmosphere, yet the *ACE*/CRIS instrument measures relatively low-energy particles (<1 GeV). The median energy (E_M) of the five selected NMs ranges from 10.17 to 12.67 GeV, corresponding to the geomagnetic cutoff rigidity of 0.30 ~ 4.58 GV. The different responses of GCRs in space and at the ground level to varying solar activity may arise from the distinct modulation processes between high and low energy particles as they propagate in the heliosphere. We infer that in the solar minimum $P_{24/25}$, the low-energy GCR particles are more likely to be influenced by the weakening solar mod-ulation compared to the high-energy particles. In addition, the NM count rates are sensitive to the complex changes in the Earth's environmental fluctuations, such as the atmospheric pressure, atmo- spheric temperature, atmospheric water vapor, instrumental temperature, dynamic magnetospheric condition, and snow effect (see Moraal & Stoker 2010, and references therein). The accurate reason

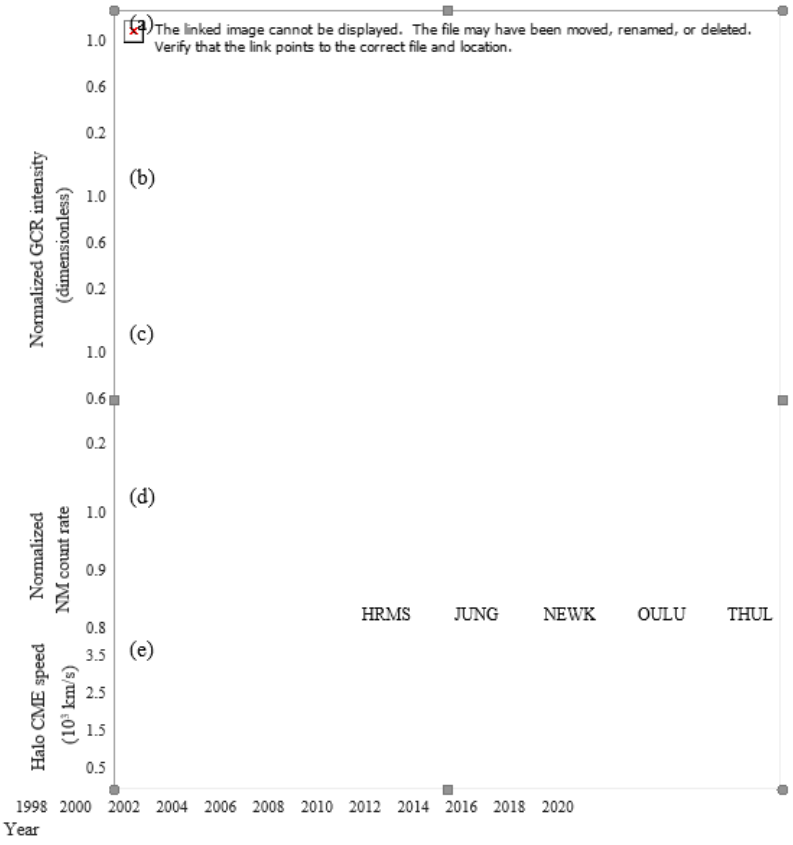

Figure 4. *Inner Heliospheric Environment during the Solar Cycle 24*

International Journal of Electrical and Electronics Engineers
Volume 15, Issue No. 02, July-Dec 2023
ISSN (O) 2321-2055
ISSN (P) 2321 -2045

(a) Pro/CRIS GCR powers of component oxygen at seven energy stretches (69.4-89.0 MeV/nuc, 91.0-122.5 MeV/nuc, 124.0-150.3 MeV/nuc, 151.6-174.9 MeV/nuc, 176.0-197.3 MeV/nuc, 198.3-218.0
MeV/nuc, 219.1-237.9 MeV/nuc). (b) Pro/CRIS GCR powers of twelve chose GCR species (C, O, Ne, Mg, Si, S, Ar, Ca, Ti, Cr, Fe, Ni). (c) Normal forces of the twelve chose GCR species. (d) Neutron screen count rates. (e) Authentic corona CME occasions. Note that the powers in boards (a)- (d) are standardized to their sun oriented least P23/24 levels, and the flat run line addresses the standardized worth equivalent to 1. The pink-bolt dunk in the GCR power was brought about by CMEs (see Subsection 3.4 for subtleties).

for the distinction between GCR powers in interplanetary space and at the ground level is as yet not known totally.
Figure 4(e) plots the verifiable radiance CMEs recognized from the Huge Point and Spectrometric Coronagraph (LASCO) on the Sun oriented and Heliospheric Observatory (SOHO) mission starting around 1996. We put the conversation of this figure in Subsection 3.4.
Figures 5(a) and 5(b) show the Pro/CRIS noticed energy spectra of GCR components C, N, O, Fe, and Figures 5(c) and 5(d) show the unearthly proportions of 2019 to 2009, and 2019 to 1997, individually. During the sun oriented least P24/25, the critical upgrade in GCR power is seen at all lower and higher energies. In spite of the fact that GCR cores vary in energy groups, their force proportions are generally steady. The proportion of 2019 to 2009 is in the scope of 1.20 ~ 1.30, and the proportion of 2019 to

1997 is in the scope of 1.05 ~ 1.10. This is fundamentally incidental with the past examination, in which
the pinnacle GCR forces are more prominent by ~25% and ~6% during the sun based least P24/25 than those in the late 1997 and 2009, separately. Moreover, it ought to be noticed that the proportions at lower
energies are somewhat bigger than those at higher energies, showing that the low-energy GCRs are more delicate to the variety of sun powered tweak than the high-energy ones.
In Figure 6, we look at the ACE/CRIS 27-day found the middle value of GCR powers between the sun oriented cycles 23 and 24, with board (a) for 151.6-174.9 MeV/nuc oxygen and board (b) for 170.8-232.9 MeV/nuc iron. Strangely, the GCR powers are huge higher in the sun oriented cycle 24 than in the sun based cycle 23, for both climbing and slipping stages, which is the ideal consequence of the less dynamic Sun and debilitated sun powered regulation in the sunlight based cycle 24. Besides, the lower part of the GCR profile in the sunlight based cycle 23 is profound and wide, yet it is shallow and short-enduring in the sun powered cycle 24. The previous mirrors areas of strength for a nonstop sun oriented regulation, and the last option compares to a debilitating and brief length sun based balance.

The record-breaking GCR intensities at 1 AU in the solar minimum $P_{24/25}$ naturally raise the question of the contributing factors. A general solution to this question is to investigate the inner heliospheric conditions, including the rate of coronal mass ejection (CME), the Sun's polar magnetic

International Journal of Electrical and Electronics Engineers
Volume 15, Issue No. 02, July-Dec 2023
ISSN (O) 2321-2055
ISSN (P) 2321 -2045

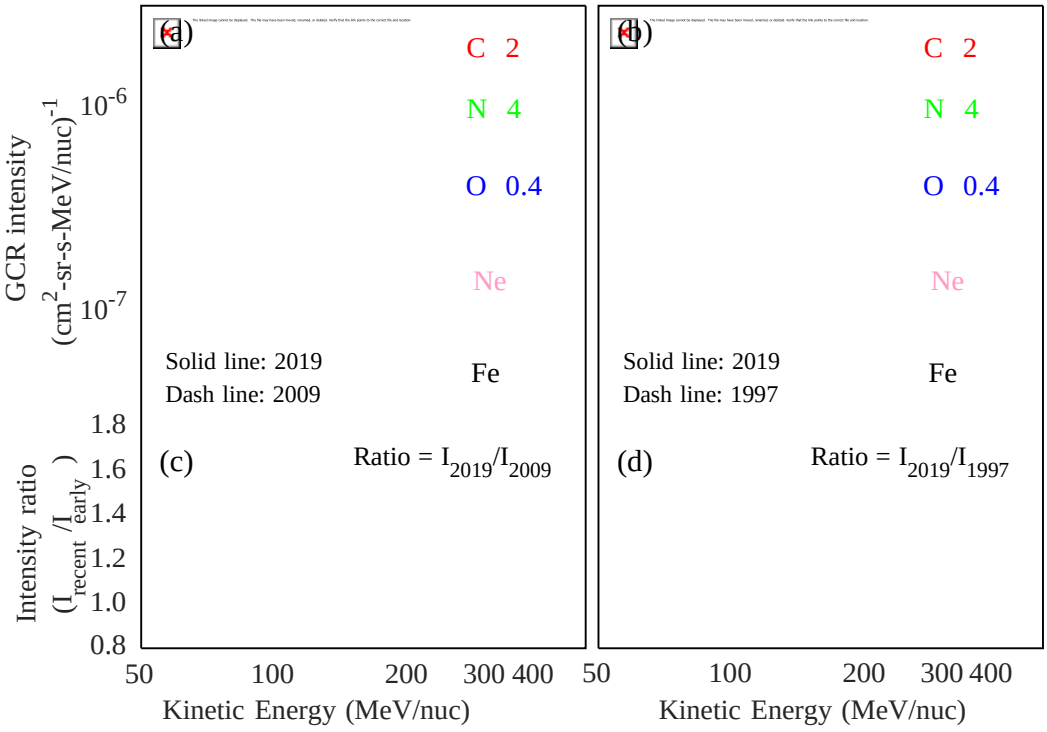

Figure 5. (a) and (b) show the examination of the ACE/CRIS GCR differential energy spectra somewhere in the range of 2019 and 2009, and somewhere in the range of 2019 and 1997, separately. Energy spectra are duplicated by inconsistent scale factor. Strong and run lines are quadratic fits to the exploratory information. (c) and (d) show the otherworldly proportions of the force somewhere in the range of 2019 and 2009, and somewhere in the range of 2019 and 1997, separately.

field strength, the slant point of HCS, the strength and disturbance of the interplanetary attractive field, as well as the speed and dynamic strain of the sun based breeze.

3.2.1. Coronal Mass Ejection Rate

CMEs normally convey more grounded attractive field than the encompassing sunlight based breeze, and cause the brutal interplanetary unsettling influences and attractive safeguarding of charged particles when the CME-driven shocks as well as attractive mists go through. Thusly, enormous CMEs actually keep grandiose beam particles from diffusing in the inward heliosphere (Wibb erenz et al. 1998; Stick 2000; Kilpua et al. 2017). In addition, CMEs are habitually went with different types of sunlight based movement, like sun powered flare (Vrˇsnak 2016; Syed Ibrahim et al. 2018), eruptive noticeable quality and X-beam sigmoids (Gibson et al. 2002; Pevtsov 2002), which further improves the safeguarding adequacy of GCR particles.

International Journal of Electrical and Electronics Engineers
Volume 15, Issue No. 02, July-Dec 2023
ISSN (O) 2321-2055
ISSN (P) 2321 -2045

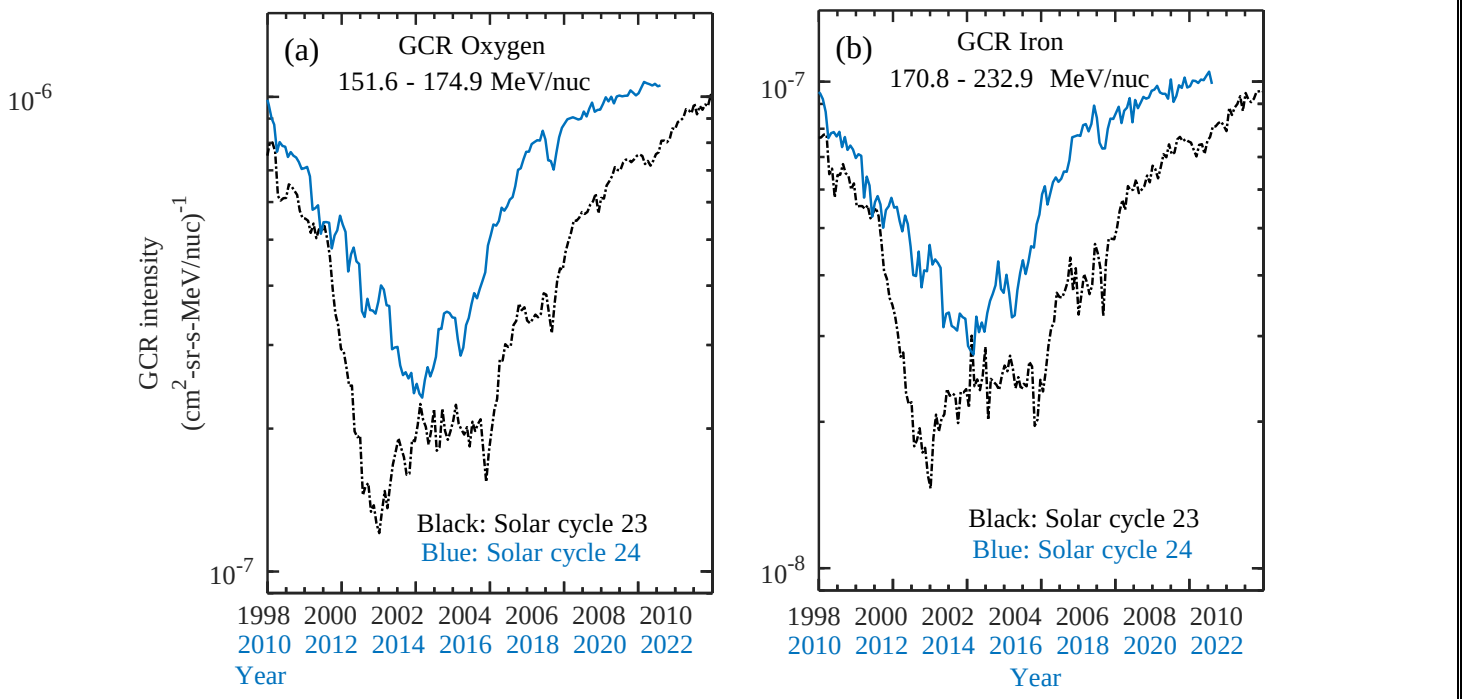

Figureq 6. Comparison of 27-day averaged GCR intensities at 1 AU between the solar cycles 23 (1998–2010) and 24 (2010–2020), for oxygen (a) and iron (b).

In Figure 7(a), we present the yearly pace of CME gained from the robotized Desert plant list somewhere in the range of 1997 and 2019. It shows that the pace of CME in 2019 is 0.29, which is ~56% and ~52% lower than that in 1997 and 2009, separately. The lower number of CMEs prompts a less attractive anomalies to hinder GCR dispersion, which thusly adds to an expansion in GCR motion. Notwithstanding the lacking number, Wang and Colaninno (2014) proposed that the speed and the mass of the CMEs in the sun based cycle 24 are a lot more modest than those in the sun oriented cycle 23. These interesting, slow speed and less gigantic CMEs somewhat debilitate the sun powered regulation of infinite beams (Paouris 2013).

3.2.2. Solar Polar Field

The extremity of the Sun's polar fields switches or flips roughly at regular intervals during the time of sun powered greatest (Babcock and Livingston 1958; Babcock 1959; Owens and Forsyth 2013). The last two inversions occur around 2001 and 2014, separately, and it is at present in the positive extremity (qA > 0). The Sun's polar fields likewise show irregular properties in the new two cycles,

International Journal of Electrical and Electronics Engineers
Volume 15, Issue No. 02, July-Dec 2023
ISSN (O) 2321-2055
ISSN (P) 2321 -2045

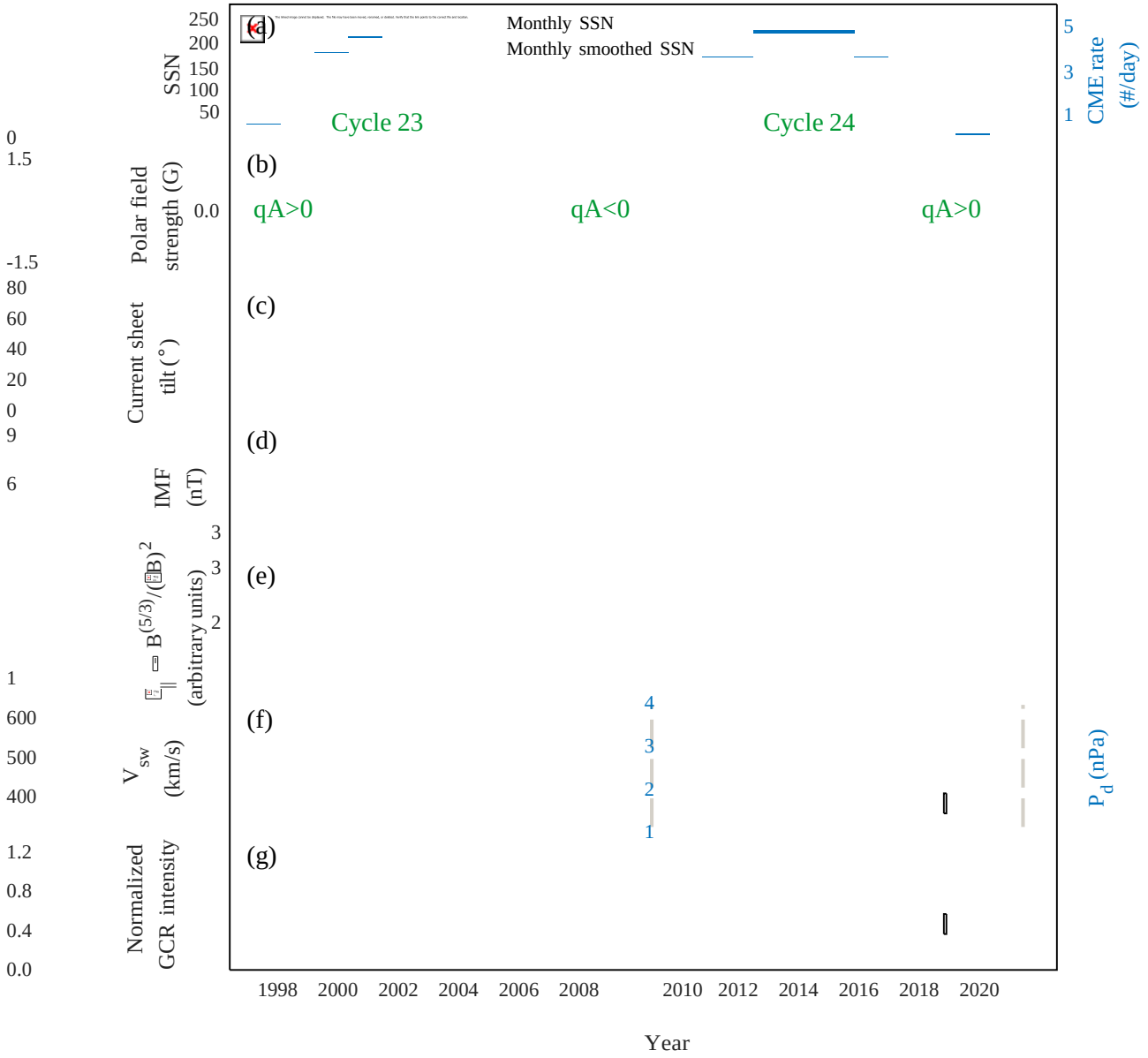

International Journal of Electrical and Electronics Engineers
Volume 15, Issue No. 02, July-Dec 2023
ISSN (O) 2321-2055
ISSN (P) 2321 -2045

Figure 7 . 27-day arrived at the midpoint of sun powered breeze/interplanetary boundaries from 1996 to 2020. (a) Sunspot number and yearly CME rate. (b) Mean sun oriented polar field strength. (c) HCS Slant point. (d) IMF greatness B and
its root mean square δB. (e) Assessed equal MFP λǁ. (f) Sun based breeze speed (dark bend) and dynamic pressure (cyan bend). (g) 69.4-237.9 MeV/nuc GCR oxygen power from Expert/CRIS (standardized to the sun based least P23/24), and the level ran line addresses the standardized GCR force equivalent to 1. The pink-bolt plunge in the GCR power was brought about by CMEs (see Subsection 3.4 for subtleties).

for instance, the discernibly debilitated polar attractive fields in the sun powered least P23/24 (Wang et al. 2009), the drawn out surprising hemispheric lopsidedness of the polar field inversion design in the sun powered cycle 24 (Sun et al. 2015; Mordvinov et al. 2016; Janardhan et al. 2018).

The Sun's polar fields impact the infiltration of GCRs into the heliosphere by changing the stream construction of the sun powered breeze and the size of the IMF (Lee et al. 2009). It is accounted for that the Sun's polar field strength in the sun based cycle 23 is ∼50% lower than that in the cycles 21-22, and the motion of the open attractive field line at the Earth circle comes to the most minimal starting around 1963 (Ahluwalia and
Ygbuhay 2010). During the sun based cycle 24, the Sun's polar field strength starts to recuperate after 2014 and goes into a level period after the year 2017 with a steady strength ∼0.6 G, which is exceptionally near or somewhat higher than that in the sun powered cycle 23, as displayed in Figures 2(b) and 7(b). It is conceivable that more GCR particles go into the heliosphere as a result of the debilitating sunlight based polar field.

3.2.3. Tilt Angle of the Helisopheric Current Sheet

Past examinations have concentrated because of a wavy interplanetary current sheet on the GCR power, and found a reverse relationship between's the HCS slant point and the GCR force (Jokipii and Thomas 1981; Potgieter et al. 2001). It is on the grounds that that the GCR particles predominantly float outward (qA > 0 extremity) or internal (qA < 0 extremity) along the HCS close to the sunlight based equator, and an enormous slant point implies that the vast beam particles need to float a more extended way length toward the Earth, prompting an expansion in the delay between the source and the spectator (Ferreira and Potgieter 2004; Mewaldt et al. 2010; Zhao et al. 2014; Ross and Chaplin 2019). The variety of the HCS slant point might have significant, even the predominant effects on the GCR tweak process during the sunlight based least age. Furthermore, the float of GCRs along the HCS assumes a more critical part than the dissemination when qA > 0.
Figure 7(c) shows the fleeting variety of the HCS slant point. The slant point starts to diminish after 2014 and arrives at the base worth of ∼2.1◦ in April 2020, which is ∼22% lower than that in
the sun oriented least P22/23 and ∼53% lower than that in the sun powered least P23/24. This very
low slant point mirrors an exceptionally near the sun powered central HCS, which brings about an upgraded outward float speed (for qA > 0) and the enormously expanded GCR force. As displayed in Figure 7(g), the HCS slant point start to build since May 2020 and arrives at a worth of 14.8◦ toward November's end
2020, joined by the continuous diminishing of the GCR transition.

3.2.4. IMF Strength and Turbulence Level

The interplanetary attractive field has significant effects on the two floats and the dispersion of the infinite beams, and the enormous beam forces are viewed as adversely related with the IMF strength (indicated by B). The float speed of the GCRs increments with the lessening of B (e.g., Jokipii and Toll 1977; Jokipii and Kota 1989). In any case, the disturbance in the IMF controls the pitch-point dispersing of the vast beams, where the dissemination coefficient of the grandiose beams is relative to 1/B or some force of 1/B (e.g., Jokipii and Davila 1981; Ferreira and Potgieter 2004).

International Journal of Electrical and Electronics Engineers
Volume 15, Issue No. 02, July-Dec 2023
ISSN (O) 2321-2055
ISSN (P) 2321 -2045

The grandiose beam dissemination related with the violent IMF incorporates both equal and opposite parts, and the connection between dispersion coefficient (κ) and molecule's sans mean way (λ) is given by:

$\lambda_{\perp,\parallel} \equiv 3\kappa_{\perp,\parallel}/v$, (1)

where v is the molecule speed, $\lambda_\parallel$ and $\lambda_\perp$ are the equal and opposite MFPs, $\kappa_\parallel$ and $\kappa_\perp$ are the equal and opposite dispersion coefficients, individually (Zank et al. 1998; Pei et al. 2010). The outspread MFP λ_{rr} represented by the equal dispersion $\lambda_\parallel$ is practically consistent inside the internal heliosphere (Zhao et al. 2017). The opposite MFP $\lambda_\perp$ is almost three significant degrees less than the equal MFP $\lambda_\parallel$ (Zhao et al. 2018). The opposite dissemination $\kappa_\perp$ is frequently expected to scale as the equal dispersion $\kappa_\parallel$ (Ferreira and Potgieter 2004).

Taking into account the standard semi straight hypothesis (QLT) and expecting magnetostatic disturbance, the equal MFP $\lambda_\parallel$ is corresponding to $B5/3/(\delta B)2$, where B is the mean IMF extent and δB is the root mean square variety in the vector IMF (Zank et al. 1998; Mewaldt et al. 2010). With the improved on connection $\lambda_\parallel \sim B5/3/(\delta B)2$, the equal MFP part $\lambda_\parallel$ at 1 AU is assessed over the cycles 23 and 24 (Figure 7(e)). The IMF greatness B arrives at the very least worth of 3.8 nT in the sun powered least P24/25, which is ∼24% more modest than that in the sun oriented least of cycles 20 to 22 (∼5 nT) yet ∼5.6% bigger than that in late 2009 (∼3.6 nT). The IMF choppiness δB is ∼2.1 nT in the sun based least P24/25, which is ∼5% higher than that in the sun powered least P23/24. The feeble IMF strength and disturbance lead to a perceptible expansion in the assessed enormous beam MFP ($\lambda_\parallel$), and the greatest worth of $\lambda_\parallel$ in the sun powered least P24/25 surpass those in 1997 by ∼31% and those in 2009

by ∼10%. It is seen that the unmistakable top on the $\lambda_\parallel$ profile (around Walk 2020) is trailed by the record-breaking GCR force.

3.2.5. Solar Wind

The sun based breeze condition (counting rate, thickness, and temperature) shifts over the long haul and impacts the GCR transport all through the heliosphere. The SW speed influences both the outward convective pace of GCRs and the adiabatic energy misfortune rate, and by and large, low sun based breeze speed decreases the outward convection rate and the adiabatic cooling energy misfortune rate. The GCR powers are viewed as anticorrelated with the sun oriented breeze speed, which uncovers that the lower the sun based breeze, the higher the GCR forces as well as the other way around (e.g., Ihongo and Wang 2016; Zhao et al. 2014).

Figure 7(f) shows the transient variety of the SW speed (Vsw, dark bend) and the SW dynamic pressure (Pd, blue bend). The typical paces during the last three sun oriented minima periods are 371 ± 19 km/s, 363 ± 26 km/s, and 374 ± 24 km/s, individually, and the relating dynamic tensions are 2.4 ± 0.2 nPa, 1.5 ± 0.1 nPa, and 1.8 ± 0.1 nPa, separately. Obviously in the sun based least P23/24, the SW speed and dynamic strain arrive at their least qualities over the beyond three sunlight based minima, which is believed to be a significant justification for the surprising high GCR powers in late 2009 (Leske et al. 2013; Zhao et al. 2014). Conversely, the improved SW speed and dynamic tension in the sun powered least P24/25 are not helpful for the increment of GCR power partially.

3.3. A Sudden Dip in the GCR Intensity during the Descending Phase of Cycle 24

During the plunging period of the sun powered cycle 24, the GCR force saw at 1 AU happens a brief span however critical dunk in the final part of 2017 (around September), after which the GCR force keeps on rising. This plunge is additionally recorded by the ground-based NM stations, as set apart by the pink bolts in Figures 4 and 7.

The sunlight based breeze and interplanetary aggravations are normally viewed as the reasons for this GCR oddity. The progressive CMEs between September 4 to 10, 2017 (remembering the quickest corona CME for 10 September 2017, see Figure 4(e)) lead to a profoundly upset interplanetary and geospace climate (Guo et al. 2018; Lee et al. 2018; Ding et al. 2020). Besides, the expanded sunspot

International Journal of Electrical and Electronics Engineers
Volume 15, Issue No. 02, July-Dec 2023
ISSN (O) 2321-2055
ISSN (P) 2321 -2045

number (Figure 7(a)), the raised HCS slant point (Figure 7(c)) and the sped up (Fig-ure 7(f)) may likewise bring about a drop in the GCR force as a result of the improved sunlight based tweak.

GCR Radiation Dose Rate on the Lunar Surface

The profound space radiation climate, comprising of sun powered and cosmic vast beams, represents an extraordinary danger to the monitored space missions. In this way, the long haul and the transient radiation impacts should be viewed as prior to planning a profound space mission. As a steady foundation of the fiery particles, GCRs are the most challenging to safeguard against and can make extreme perils space travelers and accuracy payloads on shuttles. Schwadron et al. 2010 recently revealed that the GCR portion rates close to the lunar surface during the delayed sun oriented least P23/24 are the biggest since the year 1987. Taking into account that the pinnacle worth of the GCR powers in the sun based least P24/25 is a lot higher than that in the 2009 sun oriented least, we normally need to understand what the space radiation climate is like at this point.

The Vast Beam Telescope for the Impacts of Radiation (Cavity) instrument on board the Lunar Observation Orbiter (LRO) was expected to research the lunar radiation climate, and is presently circling the Moon at an elevation of 50 km (Spence et al. 2010). Since its send off on June 18, 2009, LRO has been estimating the lunar radiation climate for almost 12 years. Figure 8 shows the hourly and everyday typical portion rates saw by the LRO/Pit, and the level scramble dabbed line is the pinnacle worth of portion rates in the sun oriented least P24/25. It tends to be seen that the portion rates are firmly related with the sunlight based movement as well as the GCR powers. In the new sunlight based least, the GCR radiation portion rate and the GCR force increment significantly in view of the debilitating sun powered regulation. We find that the pinnacle worth of portion rates in the primary portion of 2020 is ~5% higher than that in 2009-2010, which fundamentally relates to the ~6% increment in the GCR powers estimated at 1 AU. We construe that this might be the most elevated portion rates on the lunar surface since the 1980s, which advances higher prerequisites for radiation safeguarding and assurance in the space. Our outcome can be utilized to mimic the GCR space radiation chance to people in

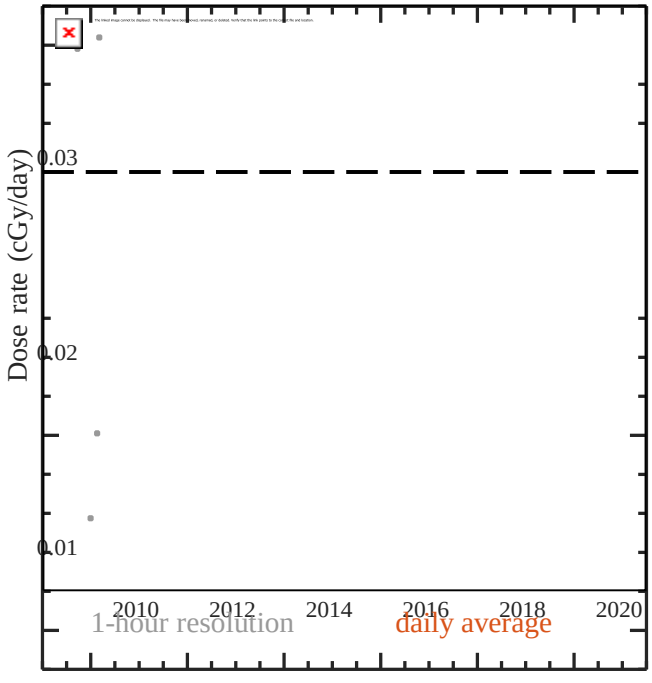

Figure 8. GCR radiation portion rates on the lunar surface estimated by the LRO/Pit. The flat scramble dabbed line denotes the pinnacle worth of rates in the sunlight based least P24/25.

the close Earth space, and give a specific reference esteem in planning the space apparatus materials in future profound space investigation missions.

4. CONCLUSIONS

The Sun was exceptionally calm during the as of late complete sun powered cycle 24, including extremely low sunspot numbers, very level heliospheric current sheet, decreased CME emission rate, frail interplanetary attractive field and disturbance level. The noticed cosmic astronomical beam powers (both in interplanetary space and at the ground level) are delicate to the heliospheric conditions, the supposed sun based regulation. In this work, we center around the varieties of the GCR powers for the period from 1997 through 2020 with estimations from the Pro/CRIS instrument, and examine the impact of inward heliospheric conditions on the GCR powers. Moreover, the drawn out varieties of the ground-based NM count rates are likewise contemplated. The ends are summed up as follows.

(1)The GCR powers saw at 1 AU arrive at the most elevated levels in the sun oriented least P24/25
since the send off of Expert space apparatus, which is ∼25% higher than that in the sun powered least P22/23 and ∼6% higher than that in the sun oriented least P23/24. With the expansion of Demon - 8 estimations and BON2020 mathematical recreation results, we observe that the GCR powers during the new sunlight based least are at the most significant levels since the space age, having the molecule energy from tens to a few hundred MeV/nuc. The record-breaking GCR powers at 1 AU increment the radiation portion rates close to the lunar surface by ∼5% in contrast with the sun based least P23/24, from the estimations of LRO/Hole instrument.
(2)The pinnacle worth of NM include rates in the sun oriented least P24/25 is lower than that in late 2009. The distinction between GCR forces in interplanetary space and NM count rates is by all accounts applicable to the different regulation cycles of the great and low energy particles. We feel that the high-energqqqqqy GCR particles are not intensely balanced as the low-energy ones, and that implies the low-energy GCR particles are bound to be impacted by fluctuating sunlight based regulation. A substitute or extra chance is that the NM count rates are delicate to the states of the World's magnetosphere and climate. It stays to be additionally concentrated on in a future work.
(3)We track down that during the sun powered least P24/25, the mean sun oriented polar field strength stays feeble and is near the worth in the 2009 sun based least; the HCS slant point arrives at any rate worth of
∼2.1◦ in April 2020, which is ∼22% lower than that in the sunlight based least P22/23 and ∼53% lower
than that in the sunlight based least P23/24; the CME emission rate is tiny, which is not exactly 50% of the CME rate during the sun powered minima P22/23 and P23/24; the strength and choppiness of IMF keep at generally low levels, which causes a ∼10% increment in the assessed astronomical beam MFP (λǁ)
contrasted with that in late 2009. This large number of variables altogether add to less sun based regulation and uncommon expansion in the GCR power.
This study is an unadulterated measurable examination of the GCR varieties in the moderately low energy band (50-500 MeV/nuc). In the in the mean time, we talk about the strange heliospheric conditions in the inward heliosphere to make sense of our discoveries of the record-breaking GCR forces at 1 AU. The amount of the heliospheric changes impact the GCR forces should be contemplated. Further work

incorporates the quantitative finding of the impacts of floats, dispersion, and convection on the astronomical beam tweak according to the point of view of mathematical reenactment (e.g., Strauss and Potgieter 2014; Zhao et al. 2014; Shen and Qin 2018; Shen et al. 2019).
q

REFERENCES

1. Aharonian, F., Akhperjanian, A. G., Bazer-Bachi,A. R., et al. 2007, A&A, 464, 235

2. Aharonian, F., Akhperjanian, A. G., Bazer-Bachi,A. R., et al. 2011, A&A, 531, C1
3. Ahluwalia, H. S. & Ygbuhay, R. C. 2010, in 12th International Solar Wind Conference, 1216, 699
4. Babcock, H. D. & Livingston, W. C. 1958,Science, 127, 1058
5. Bieber, J. W. 2013, Centenary Symposium 2012:Discovery of Cosmic Rays, 1516, 234
6. Chapman, G. A., de Toma, G., & Cookson, A. M.2014, SoPh, 289, 3961
7. Cummings, A. C. & Stone, E. C. 2007, TheComposition of Matter, 389
8. Ding, Z. Y., Li, G., Hu, J. X., et al. 2020, Researchin Astronomy and Astrophysics, 20, 145
9. Ferreira, S. E. S. & Potgieter, M. S. 2004, ApJ,603, 744
10. Fu, S., Jiang, Y., Airapetian, V., et al. 2019,ApJL, 878, L36
11. Fu, S., Zhao, L., Zank, G. P., et al. 2020, Science China Physics, Mechanics, and Astronomy, 63, 219511
12. Giacalone, J., Drake, J. F., & Jokipii, J. R. 2012, SSRv, 173, 283
13. Gibson, S. E., Fletcher, L., Del Zanna, G., et al.2002, ApJ, 574, 1021
14. Gloeckler, G., Fisk, L. A., Geiss, J., et al. 2009, From the Outer Heliosphere to the Local Bubble, 163
15. Gonçalves, Í. G., Echer, E., & Frigo, E. 2020,Advances in Space Research, 65, 677
16. Guo, J., Dumbović, M., Wimmer-Schweingruber,
17. R. F., et al. 2018, Space Weather, 16, 1156Hajra, R. 2021, SoPh, 296, 33
18. Hasebe, N., Kondoh, K., Mishima, Y., et al. 1997,Advances in Space Research, 19, 813
19. Hovestadt, D., Vollmer, O., Gloeckler, G., et al.1973, PhRvL, 31, 650
20. Hu, J., Li, G., Ao, X., et al. 2017, Journal of Geophysical Research (Space Physics), 122, 10,938
21. Hu, J., Li, G., Fu, S., et al. 2018, ApJL, 854, L19
22. Ihongo, G. D. & Wang, C. H. T. 2016, Ap&SS,361, 44
23. Jämsén, T., Usoskin, I. G., Räihä, T., et al. 2007, Advances in Space Research, 40, 342
24. Janardhan, P., Fujiki, K., Ingale, M., et al. 2018,A&A, 618, A148
25. Jiang, J. & Cao, J. 2018, Journal of Atmosphericand Solar-Terrestrial Physics, 176, 34
26. Jokipii, J. R. & Kota, J. 1989,Geophys. Res. Lett., 16, 1
27. Jokipii, J. R. & Davila, J. M. 1981, ApJ, 248, 1156Jokipii, J. R. & Thomas, B. 1981, ApJ, 243, 1115
28. Kilpua, E., Koskinen, H. E., & Pulkkinen, T. I.2017, Living Reviews in Solar Physics, 14(1), 5

29. Kóta, J. 2013, Space Science Reviews, 176, 391 Kuznetsov, N. V., Popova, H., & Panasyuk, M. I.
30. 2017, Journal of Geophysical Research (Space Physics), 122, 1463
31. Lave, K. A., Wiedenbeck, M. E., Binns, W. R., etal. 2013, ApJ, 770, 117
32. Lee, C. O., Luhmann, J. G., Zhao, X. P., et al.q2009, SoPh, 256, 345
33. Lee, C. O., Jakosky, B. M., Luhmann, J. G., et al.2018, Geophys. Res. Lett., 45, 8871
34. Leske, R. A., Cummings, A. C., Mewaldt, R. A.,et al. 2013, SSRv, 176, 253
35. McDonald, F. B., Teegarden, B. J., Trainor, J. H.,et al. 1974, ApJL, 187, L105
36. McDonald, F. B., Webber, W. R., & Reames,
37. D. V. 2010, Geophys. Res. Lett., 37, L18101 Mertens, C. J. & Slaba, T. C. 2019, Space Weather, 17, 1650
38. J. R., et al. 1993, Geophys. Res. Lett., 20, 2263 Mewaldt, R. A., Davis, A. J., Lave, K. A., et al.2010, ApJL, 723, L1
39. Mishev, A. L., Kocharov, L. G., & Usoskin, I. G.2014, Journal of Geophysical Research (Space Physics), 119, 670
40. Moraal, H. & Stoker, P. H. 2010, Journal ofGeophysical Research (Space Physics), 115,A12109
41. Mordvinov, A., Pevtsov, A., Bertello, L., et al.2016, Solar-Terrestrial Physics, 2, 3 Owens, M. J. & Forsyth, R. J. 2013, Living Reviews in Solar Physics, 10, 5
42. Parker, E. N. 1965, Planet. Space Sci., 13, 9 Pei, C., Bieber, J. W., Breech, B., et al. 2010,Journal of Geophysical Research (Space Physics), 115, A03103
43. Potgieter, M. S., Burger, R. A., & Ferreira,S. E. S. 2001, SSRv, 97, 295
44. Ross, E. & Chaplin, W. J. 2019, SoPh, 294, 8 Sabbah, I. 2000, Geophys. Res. Lett., 27, 1823 Schwadron, N. A., Boyd, A. J., Kozarev, K., et al. 2010, Space Weather, 8, S00E04
45. Thomas, S. R., Owens, M. J., & Lockwood, M.2014, SoPh, 289, 407
46. Tylka A. J., Adams J. H.,Boberg P. R., et al.,1997, IEEE Trans. Nucl. Sci. 44, 2150
47. Upton, L. A. & Hathaway, D. H. 2018,Geophys. Res. Lett., 45, 8091
48. Usoskin, I. G., Braun, I., Gladysheva, O. G., et al.2008, Journal of Geophysical Research (Space Physics), 113, A07102
49. Wang, Y. M., Robbrecht, E., & Sheeley, N. R.2009, ApJ, 707, 1372
50. Wang, Y. M. & Colaninno, R. 2014, ApJL, 784,L27
51. Wibberenz, G., Le Roux, J. A., Potgieter, M. S.,et al. 1998, SSRv, 83, 309

52. Zank, G. P., Matthaeus, W. H., Bieber, J. W., Moraal, H. 1998, Journal of Geophysical Research: Space Physics, 103, 2085

53. Zhao, L. L. & Qin, G. 2013, Journal of Geophysical Research (Space Physics), 118,1837

54. Zhao, L. L., Qin, G., Zhang, M., et al. 2014, Journal of Geophysical Research (Space Physics), 119, 1493

55. Zhao, L. L. & Zhang, H. 2015, ApJ, 805, 6 Zhao, L. L. & Zhang, H. 2016, ApJ, 827, 13

56. Zhao, L. L., Adhikari, L., Zank, G. P., et al. 2017,ApJ, 849, 88

57. Zhao, L. L., Adhikari, L., Zank, G. P., et al. 2018,ApJ, 856, 94

58. Zhao, L. L., Zank, G. P., Hu, Q., et al. 2019, ApJ,886, 144